Power flow control in a substation of a wind- and solar farm

BSc. Graduation Thesis

Group 09.01

F.G.N. Rimon, 4652827
M. Mastouri, 4599470

TUDelft

Power flow control in a substation of a wind- and solar farm

BSc. Graduation Thesis

by

Group 09.01

F.G.N. Rimon, 4652827
M. Mastouri, 4599470

TUDelft

Abstract

Renewable energy generation is nowadays increasing around the world, especially wind- and solar power generation. However, increasing wind and solar power integration into the grid has a significant effect on the power system. The variability and uncertainty of these energy sources proposes new challenges for companies involved in grid management. In order to face these challenges, advanced control schemes and optimization algorithms has to be implemented in order to ensure stability and efficiency of the power flow. But these algorithms can only be implemented if the power flow in the system is modeled accurately. This thesis explains how the power flow in a substation of a wind- and solar farm in Zeewolde, the Netherlands, is modeled in order to guarantee efficiency and stability.

Preface

The scope of this thesis is to provide an accurate model of the power flow in a substation with renewable energy sources, the Zeewolde wind-and solar park. The thesis is part of a project given by ABB. ABB aims to use this model as a complementary solution to satisfy TSO requirements at the point of common coupling with minimal losses in power and maximum stability. We would like to thank our supervisor dr. ir. José Rueda Torres for his exceptional guidance throughout the project. In cooperation with José, we were able to iteratively formulate requirements that would satisfy a realistic representation of the substation. Especially, dr. ir. José made an effort in providing the best quality of guidance under the COVID-19 circumstances. Furthermore, our gratitude is expressed for Dennis Groenenberg and Jan who constantly provided us with the information of the Zeewolde park needed for fulfillment of the scope of the project. Lastly, the complete project would not have been possible without the help of our colleagues, Alexandru Neagu, Dennis Groenenberg, Jin Han Bai and Laurens Beijnen. Because of you, the motivation stayed high while being in an enjoyable online atmosphere.

Group 09.01

F.G.N. Rimon, 4652827
M. Mastouri, 4599470

Delft, May 2020

Contents

1

Introduction

In the past decade, the renewable energy market has increased significantly [22]. Equivalently, the current methods for energy provision such as coal, are becoming less popular. Ongoing research has the aim to make the transition to renewable energy as safe (f.e., no overloading) and efficient (f.e., no transmission losses) as possible [2].

1.1. Project objective

Ideally, once the substation is connected to the grid, the substation provides its full capacity at all times. However due to fluctuations in wind- and solar profiles, the Transmission System Operator (TSO) requirements cannot always be satisfied at the Point of Common Coupling (PCC) [12]. There is also loss in several of the components which form the subsystem such as power loss in the transmission lines, bus bars, transformers and even in the Wind Turbine Generators (WTGs) and PV panels. Since these losses will effect the power generated and the power delivered at the Point of Common Coupling, they have to be taken into account in order to implement an accurate model for the system.

In the stator rotational energy of the blades of the wind turbines is converted into electrical energy. Since the conversion is made with magnets, AC current production occurs. This gives rise to different AC voltages on the nodes of the power system of the wind modules. These voltages can be lagging or leading to the current in the power system, which gives rise to either absorbing or generating reactive power by the wind turbines. However, at the nominal value of 1 p.u, the voltages will not be lagging or leading, but in phase with the current, which will result in no reactive power. One of the requirements of the Transmission System Operator is to control the reactive power and assure that, when needed, the reactive power at the Point of Common Coupling is brought to zero.

The power in the PV module is generated in DC conditions. Hence, the solar modules do not generate any reactive power. Since the transmission grid operates in AC conditions, the DC power has firstly to be converted to AC in order to be fed back into the grid. For this conversion process, DC/AC inverters are used. These inverters will either generate or absorb reactive power **??**. This reactive power has to be taken into account in order to design an accurate as possible solar farm.

In addition, advanced control schemes are designed to find the optimal setpoints in the substation that satisfy TSO requirements. The setpoints indicate the power flow through each generation string. The optimisation is based on the system's configuration and non-idealities, but also on the grid code requirements [1]. This mathematical scheme cannot determine the feasibility of the given setpoint in reality. It needs information of the substation's power flows. Through communication between the modeling and optimization entity, the scheme can make its search space smaller and find a global optimum.

The project aims to use the case study, shown in Fig. 1.1, to design an accurate model of the power flows

---

[1] "Grid codes specify the electrical performance that generation assets must comply with in order to obtain the required approval for its connection to a grid."[7]

that shows the effects of fluctuating wind/solar profiles and components' non-idealities. When the optimization algorithm sends setpoints to the model, the model returns the actual feasibility by providing the power flows in each of the branches in the system configuration. Dependent of the development status of a project, this model can indicate if the system configuration is to be improved/changed. Additionally, it provides the feasibility for future expansion of the substation without violating any physical constraints. Steadily, increasing the RES generation for the growing energy demand worldwide.

For the scope of this project, a realistic model of the system behaviour shall be designed and tested. The models for the PV- and WTG farm of the case study are combined and tested under critical conditions, such as low wind speed, low solar irradiance, or both for high reactive power requests from the TSO. The problem formulates: "When is the system able to satisfy high load demands at the PCC under critical, i.e. too low or too high, generation of power from the renewable energy systems?"
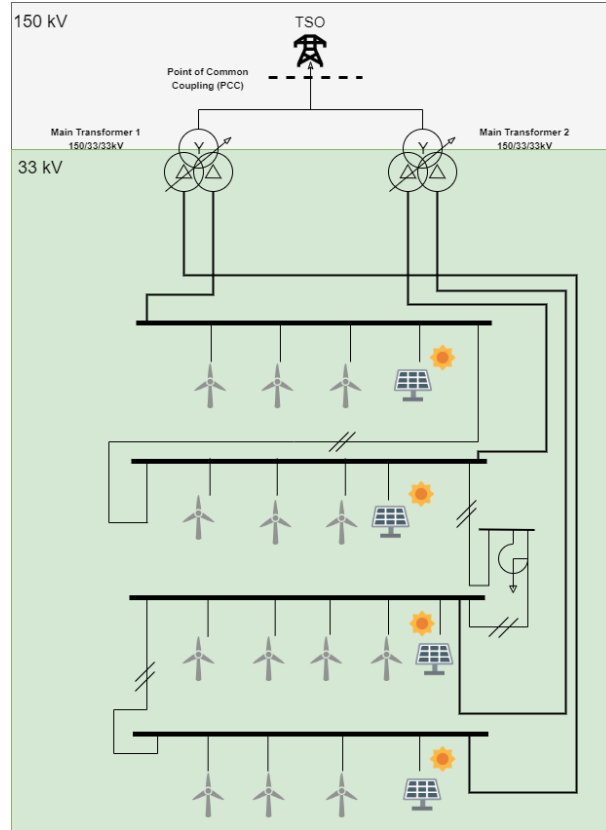
Figure 1.1: Simplified schematic of case system

1.2. Test models and state-of-art

In order to perform several power system analysis, information about the power system is needed, which consists of the system topology and nodal power injections. The nodal power injections consist of active- and reactive power, which are either measured or determined. In Fig. 1.2 the input and output data of an iterative power flow calculation is shown.

Furthermore, in the iterative power flow calculation block certain equations are applied. The generic equation, as shown in Eq. 1.1, will be used in order to generate the voltage magnitude p.u and angle of all nodes iteratively. However, there is one bus, frequently allocated to the bus at the PCC, for which the voltage magnitude p.u and angle are known. This bus is called the slack bus. In this bus the active and reactive power injections are determined with the known voltage magnitude p.u and angle in order to check whether certain requirements at the PCC are fulfilled. In the remaining nodes the voltage magnitude p.u and angles of the busses will be determined with the known values of the active and reactive power injections. These busses

Figure 1.2: Block diagram with the input and output data in order to perform power flow calculations.
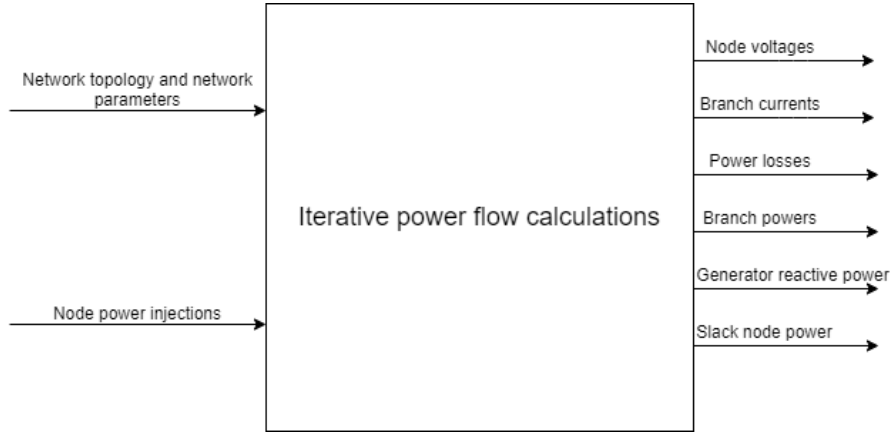
are called PQ-busses and are used since they give rise to a set of finite equations, which will result in a finite number of solutions for the magnitudes and angles. For the PQ-busses, there are in principle two equations generated, one for the active power and one for the reactive power, as shown in Eq. 1.2 and 1.3. Since the unknown variables in all PQ-busses are the voltage magnitudes p.u and angles, a state variable matrix $\mathbf{x}$ can be constructed, as shown in Eq. 1.4, from which all the PQ-busses can be solved iteratively by solving Eq. 1.5.

$$I_{[Nx1]} = Ybus_{[NxN]} \cdot U_{[Nx1]} \tag{1.1}$$

$$P_i = f_p(U_1, U_2, ..., U_N, \delta_1, \delta_2, ..., \delta_N) \tag{1.2}$$

$$Q_i = f_q(U_1, U_2, ..., U_N, \delta_1, \delta_2, ..., \delta_N) \tag{1.3}$$

$$\mathbf{x} = [\delta \, U]^T \tag{1.4}$$

$$f(\mathbf{x}) = 0 \tag{1.5}$$

Different algorithms have been designed to solve $\mathbf{x}$ in Eq.1.5 in an iterative manner. Reason for more algorithms are its solving (or convergence) time and accuracy for specific networks. These modern algorithms still make use of the two conventional approximation methods, Gauss-Seidel method [10] and Newton Raphson method [19]. Gauss-Seidel is a simpler technique requiring less computation per iteration. The computation time is sensitive to the system parameters. Therefore, the majority bases the algorithm on Newton-Raphson, since the system converges in less iterations, which gives smaller computation time, more accuracy and makes it less sensitive to other system parameters. This makes it suitable for a complex system, as shown in Fig. 1.1. A more precise schematic is visible in App. A.1.

A fluctuation in wind/solar profile, causes a fluctuation in the power generated. Current methodology takes this fluctuation in wind/solar profiles by designing algorithms that describe a probabilistic behaviour of wind speed and solar irradiance [3] [5] [1]. This probabilistic behaviour is to test the system under the most common operating situations, i.e. common wind/solar profiles, since little variation from the rated wind speed is included to the model. Additionally, the probabilistic model offers the possibility to create both random load demands and generation capabilities in the system at random dispatches. Therefore occasionally violating physical constraints of the system. This offers a test model for alert operating conditions [2]. Hence, the probabilistic model offers a suitable test model under different operating conditions. Compared to use of historical data, which can vary throughout time periods (per season or year), this test model runs more situations.

---

[2]alert operating conditions in which physical constraints are violated or there is a high vulnerability to disturbances

To model daily wind profiles, research makes use of:

1. a Weibull distribution

2. historical data

3. a versatile distribution that combines Beta, Cauchy and Gaussian to model a daily wind profile [23]. [11]

However the majority makes use of Weibull PDF, since it was determined that the distribution resembles real life situations the most [21] [14] [11]. For solar irradiance, each research makes use of an own model. These models can be divided into:

1. Design based on historical data and chosen PDF [25].

2. Beta distribution [8] [11].

3. Weibull distribution [8].

4. Design based on spatio-temporal stochastic model with each spatio(or season such as sunny, cloudy,etc.) having own stochastic parameters[17].

Out of these models, the probability for output power is determined. This offers a solution in case of insufficient or inaccurate wind-and profile data. Other research, suggest a π- model of the individual WTGs and PV panels to determine the output active- and reactive power. It makes use of properties of the system. This provides an accurate solution if all data is known, i.e. datasheet of the WTG as well as the profile data [16] [9] [20]. For the probabilistic model of the RES, the reactive power output is unknown in case of insufficient data about the system itself.

Due to its maturity and proven performance as open source tool, Matpower was selected for the design of a model in steady state and AC conditions. MATPOWER is a MATLAB package aiming to solve steady-state power simulations [24]. For this model the basic Newton-Raphson method is used. More sophisticated methods would be possible if the system was a radial network, where each load has its own generator. The system configuration in Fig. 1.1 analyses a network system, which has multiple generating sources for a single load. Also, the sophisticated methods, are focused on reducing computation time, which is not part of the scope for this project.

The challenge for this project is to have an accurate model of the power flow for a substation that combines both wind-and solar generation under normal and extreme weather conditions. The state of art does not seem to analyse such a case study. Research does address the effects of such a substation on the transmission grid, but not on the substation. In addition, there shall be looked at the loss effects of the 3-winding transformers. These will be approximated with an equivalent 2-winding transformer model. The sub group responsible for optimisation shall find the optimal tap position and send it to the modeling subgroup. This interaction is visible in Fig. 2.1.

Due to insufficient data of both wind profile and WTG's components for the specific case study, using only one model will yield inaccurate results of the power flow. To model such WTGs under fluctuating wind profile conditions, the best model is achieved by combining both methods. The different operating conditions is tested with the probabilistic behaviour, while the PQ/RX model determines the exact output of wind modules after internal losses. Therefore, a correct estimate of the active, reactive power generation and voltage profile is formulated for each dispatch profile.
Next, the same can be done for the PV modules. The models for reactive power capability and probabilistic solar irradiance are combined. In reality, most of the time, both PV- and WTG farm will be active. All generating strings, Fig. 1.1, influence the system simultaneously in normal-and critical operating conditions. With the farm being fully active, voltage profiles can deviate a lot from the ideal 1 p.u., leading to violation of technical constraints.

1.3. Thesis outline

To formulate a correct answer for the project objective, the thesis will delve into the necessary requirements to determine what it means to have an accurate power flow model. Once requirements are determined in Chap. 2, a procedure (Chap. 3, 4) with subsequent results (Chap.5), is analysed. Out of the results, a conclusion will be made in Chap. 6 and a discussion about the results can be formulated in Chap. 7. This discussion offers room for improvement and recommendations for future researchers modeling power flows for similar case studies.

2

Programme of Requirements

2.1. Functional requirements

As mentioned in Chap. 1, to formulate a correct research, the problem shall be divided in smaller subproblems. The model should be able to:

1. Update the components' parameters in the system topology after every setpoint iteration.

2. Indicate when constraint limits of voltage and/or current are violated in each branch or bus of the substation.

3. Indicate losses and injections of each branch and bus of the system for given setpoints.

4. Take influences into account for power generation due to fluctuating wind- and solar profiles.

To determine how the model will indicate if requirements are satisfied, one needs a correct definition of setpoints received from the optimization scheme. The interaction of the subgroups is specified in Fig. 2.1. The interaction between the three components of the optimisation unit is found in App. A.3. For the case study, the setpoints will be given in the form a dispatch vector, which indicates the required reactive power from the generating strings, 13 WTG strings and 4 PV strings, shown in Fig. A.1. Additionally, the connection status for the reactor is required. Usually the reactor is disconnected, but if the optimization scheme requires this in order to satisfy reactive power at the PCC, the reactor will absorb reactive power (-12 MVAr).
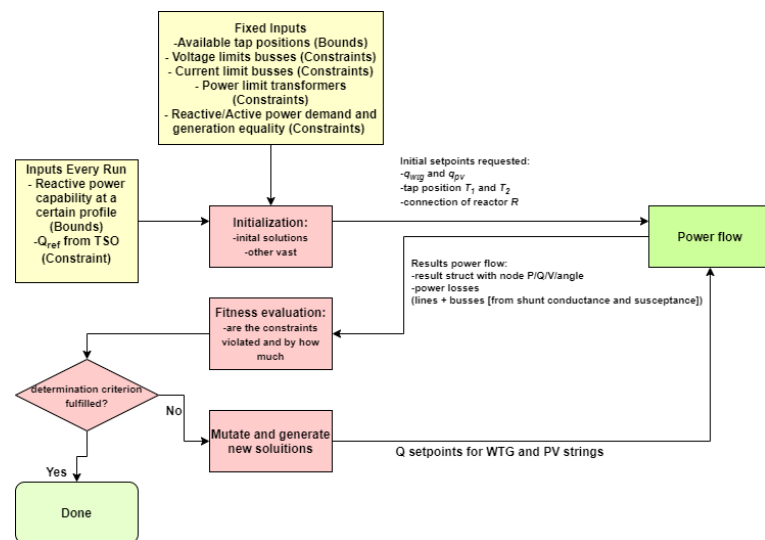

Figure 2.1: Interaction between optimization and modeling of the power flows

2.2. Model requirements

The sub problems are formulated in Mandatory requirements, Trade-off requirements and optional requirements. Mandatory requirements are:

1. To take the influence of each component in the system into account:

    (a) Formulate a system topology which connects each node of App. A.1. Hereby, all information of the system is implemented. This includes the PCC, wind- and solar PV strings, transformer- and cable data.

    (b) The design of the solar farm. This overview consists of the interconnection of the solar modules, the cable types and the type of DC/AC converters used.

    (c) To determine the reliability of the implemented case system, power flows are compared to own hand calculations that apply the theoretic approach [19].

    (d) After completion of the first two requirements, the system topology is formulated on string level. Hereby, the system topology is updated with the subdivision of individual WTGs at each string. Each WTG has its own rated power output, cable and inverter type connection. More will be explained in Subsec. 3.2.1.

2. To determine the system behaviour for every possible operating condition:

    (a) An analysis of the system behaviour for different operating conditions. From this, the relation is determined between total losses, injections and voltage profiles for each combination of generation and demand. This includes extreme combinations for which the power demand will not only come close to generated power, but also exceed generation of the strings.

    (b) An analysis on the behaviour of components that cause most voltage physical violations and losses.

3. For proper communication between the requests of the optimization controller and the model:

    (a) The system topology has to be updated twice after each given setpoint. The first update is to change the active and reactive power generation according to the wind and solar dispatch. The second update is to change the the reactive power of the generation strings.

    (b) Before receiving setpoints from the optimization scheme, the available active and reactive power, with tap positions from each transformer is sent to the optimization scheme. With this information and system, the optimization scheme can determine the initial vector of string setpoints.

The satisfaction of mandatory requirements can be tested once the system converges on MatPower for a Newton Raphson power flow [24], after the system parameters are updated or sent to the optimization scheme.

Trade-off requirements are necessary in order to improve the research in a stepwise manner. This results in conclusions that can be used for future expansion of the case study used, since its behaviour is modelled for every possible conditions. Therefore, trade-off requirements are:

1. Include losses generated by changing the tap position of the equivalent model of the 3-winding transformers. This tap position is updated in the system topology according to the procedure in Fig. 2.1.

2. Include losses generated by the equivalent model of the 3-winding transformers' inner-and outer winding in the transmission lines.

Furthermore, there are also optional requirements, which are not needed to design, implement and test the model, but can be implemented in the future in order to add new insights to the research, namely:

1. Design the PQ and RX models used in state of the art research in order to model the PQ-capability curves of the wind turbines [16]. However, for this research the PQ-capability curves of the WTG's were available [15] and no data is supplied about the impedances of the rotor and stator of the WTG's. This resulted in considering the implementation of the PQ and RX models as an additional requirement. In a later phase, the PQ and RX models could be designed using data from other researches in order to give an as accurate as possible estimation of the PQ-capability curves. Eventually, these estimations can be used in order to give a comparison between two different modeling methods.

Additional requirements are needed for the proof of concept. Hereby, the design of a visualization model for the Single Line Diagram of the case study, with the power flow and losses indicated after every system update [15]. Note: For the prototype, it is not of importance which component, i.e. cable or transformer, generates the loss.

Concluding, once mandatory requirements are satisfied, the model will prove to be accurate for power control at the PCC, because it includes transmission losses and most importantly, the behaviour of the wind-and PV modules for rated power output. In addition, trade-off requirements will supplement the model by testing the system configuration under different situations determined by the probabilistic behaviour. Furthermore, optional requirements firstly add a new level of accuracy to the model, since additional losses in the farms are accounted for. Secondly, they could give new insights to research, since results of state of the art models are compared with the results of the models used in this research. Additionally, losses of previously ideally assumed components are included, providing actual power flow in the system topology.

3

Model of the system configuration

For the design of the model, the data in [15] [13] was used. This offers the configuration with assigned bus numbers, cables', transformers' type and length shown in Fig. 3.6. Here, the rightmost generation string of bus bar 7,12,16,23 are the PV strings. In App. A.1, the system configuration is shown with maximum voltages for bus bars and maximum current for branches. On the left, the base voltage is indicated for each section of the substation.

Since [15] offered insufficient data of capability curves of the WTG and PV- farm, certain assumptions were made. Firstly, it was decided to make the slack node the PCC, i.e. bus bar 1. The voltage magnitudes and angles of each bus were compared to the PCC node, with a magnitude of 1 p.u. and 0 degrees. To implement the constraints for the voltage profile, it was decided to determine this from the main transformer data. The transformer data indicates the maximum input/output voltage and current. These values are shown in Tab. 3.1. Although the cable type can handle more, the main transformers set the power flow limits for the system configuration.

3.1. Cable modeling

Different branches in the system topology had different three-phase configurations. It was decided to model this configuration, using an equivalent π transmission line model. In Fig. 3.1, each branch will have a starting node, i.e."Bus from", and ending node, i.e."Bus to". The branch between these nodes has a series impedance, Z_s, consisting of a real and imaginary impedance. The injection charge of busses is modelled with a parallel charging susceptance, b_c. Some of the branches are transformers. To specify this in a systematic manner, each branch has a transformer with a tap ratio, i.e. **N**. For most branches this ratio is equal to 1. The phase shift, θ between nodes is unknown and therefore considered to be its ideal value of 0.

To calculate the π model values for each branch of the system in Fig. 3.6, the cable type and configuration were determined. The DC resistance value for a nominal temperature of 20 degrees Celsius was assumed. The configuration is specified with AxBxCCxD mm2 "material". **A** specifies the amount of cables per single phase. **B** specifies the amount of phases, i.e. in this system it is a three-phase system for each node. **C** specifies the amount of parallel cables in one single phase cable. The extra C stands for "cable", indicating where the single phase specification commences. **D** specifies the cross-section area of the cable in mm2. An example of the configuration is shown in Fig. 3.2. Diagrams of other configurations are found in App. A.2.1.

After specification of the cable configuration, the parameter values are calculated to per unit to have a more uniform definition of the differences in absolute values. Tab. **??** specifies the parameter values of the branches per km. Multiplying it with the distance of the specified branch, the absolute value is obtained.

Table 3.1: System constraints based on transformer data

	V_{max} (kv)	I_{max} (A)
primary side	33	735
secondary side	171.316	808.6

Table 3.2: Absolute impedance and capacitance values per km of cable types. Data acquired from [15].

Cable	Resistance (Ohm/km)	Reactance (Ohm/km)	Capacitance (e-6 F/km)	Apparent power rate (MVA)
3x1Cx2500mm2 XLPE Al	0.0119	0.06788	0.3	400
1x800mm2 AAC Conductor	0.0356	0.101	0.366	400
2-winding transformer	0	0	0.2025	240
3x1Cx1000mm2 XLPE Al	0.0291	0.1666	0.38	46.2977
4x3x1Cx1000mm2 XLPE Al	0.007275	0.0415	1.52	185.19
3x630mm2 Cu	0.0283	0.163	0.35	36.86
3x630mm2 Al	0.0469	0.177	0.32	36.86
3x400mm2 Al	0.0778	0.19	0.26	28.29
3x240mm2 Cu	0.125	0.196	0.22	20.86
3x150mm2 Al	0.206	0.208	0.19	16.28
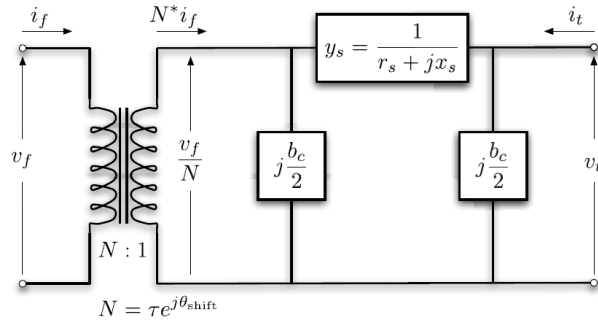
Figure 3.1: Equivalent π transmission line model for the branches of the system topology, Fig. taken from [24].

Eq. 3.2 describes the calculation of the base impedance. The base voltage is dependent of the region where the branch is, i.e. two regions. The first region is the secondary side of the transformer with a 150 kV output voltage. The second region is the primary side of the transformer with a 33 kV input voltage. For the sake of simplicity, a base power of 100 MVA is chosen for the entire transmission system. After the base impedance is calculated for the specified region, Eq. 3.3 calculates the per unit values for each branch. Similarly, the susceptance is calculated. Additionally, the apparent power rates of the branches have to be determined in order to satisfy the power limits of the system. The rated apparent power is determined using Eq. 3.1.

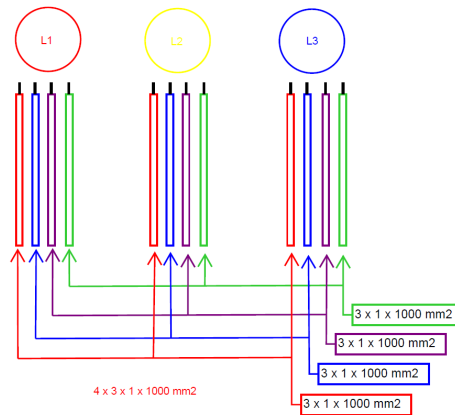$$S_{Rated} = \sqrt{3} \cdot I_{Rated} \cdot V_{Base} \tag{3.1}$$

Figure 3.2: Configuration of a branch with XLPE 4x3x1Cx1000mm2 Al cable. Data from [15].

$$Z_{base} = \frac{V_{base}^2}{S_{base}} \qquad (3.2)$$

$$Z_{perunit} = \frac{Z_{absolute}}{Z_{base}} \qquad (3.3)$$

Although all branches are modelled, there are specific branches that are considered to be disconnected unless stated otherwise by the optimization setpoints received. Firstly, **The shunt reactor** is assumed to be disconnected. Therefore, branch 12-28 and 17-28 are disconnected. Ideally, this is connected only in the case that the generating strings are unable to satisfy a specific amount of reactive power demand from the TSO. Additionally, if negative reactive power is needed in the system to prevent violations of constraints. The influence of the shunt reactor is analysed in Chap. 4.

Branch 7-12 and 17-23 are disconnected. These branches are safety branches in case of faulty conditions, i.e. overcurrent or overvoltage at the bus bars. The current will in such case be higher than 2500 A, or higher voltage than 36 kV, shown in App. A.1.

3.2. Modeling the WTG farm

3.2.1. Design of WTG on string level

3.2.2. Design of the WTG capability curve

For the WTG, there is a relation between the active output power and reactive output power. In most WTG modeling, the relation is straightforward. The WTG will provide maximum reactive power at all times. With the Enecon Type C used as example [15], this relation is shown in Fig. 3.3 for a voltage magnitude of 1 p.u. When the voltage is unequal to 1, the P-Q relation changes. In addition, some WTGs will produce maximum reactive power, once a certain active power threshold is reached. This condition is shown in Fig. 3.4.

Both cases make the modeling of the output reactive power for the WTG complex. Ideally, from the PQ/RX model, the function for the P-Q relation dependent of the voltage magnitude is calculated [16]. From this derivation the exact output and P-Q relation is determined. However, due to insufficient given data from the case study, the implementation for a PQ/RX model is not feasible. For this reason, the P-Q relation is derived from the Enecon P-Q diagrams of App. A.2 [15].

The procedure to implement the non-ideality of the P-Q relation will consist of determining the equivalent P-Q relation for each WTG generating string in App. A.2. An approximation of this P-Q relation is made by dividing the capability curve in three sections. The first section models the linear slope to reach maximum reactive power at the threshold for the active power. The second section approximates the common case of maximum reactive power. The third section will approximate the decrease of reactive power specified with the slope of a voltage of 0.9 p.u., shown in Fig. 3.4. This slope is considered to be a reliable approximation, since it is the closest to the minimum physically allowed voltage of 0.8576 p.u. This prevents a complex implementation of the P-Q relation as a function of varying voltages for each WTG string.

3.3. Design of the solar farm

3.3.1. Determination of solar farm parameters

For the design of the solar farm, there was no data supplied. This offered a degree of freedom in the design. A rule-based approach is used for the design of the farm.

Firstly, the active power generation of the solar farm is determined. The generation is determined by analysing the weak components of the system. Weak components are considered to be the components, which will give the first violations when running the powerflow. In this case study the weak components are considered to be the transformers and the cable to the PCC. In order to prove this, these components are analysed with the WTG farm generating active power at rated wind speed. The results of this analysis are shown in Figures **??**, **??** and **??**.

From Fig. **??**, **??** and **??** can be concluded that in this case system the branch to the PCC is the weakest component. As can be seen in Figure **??** a capacity of 40 MW can be added before reaching the branch limit

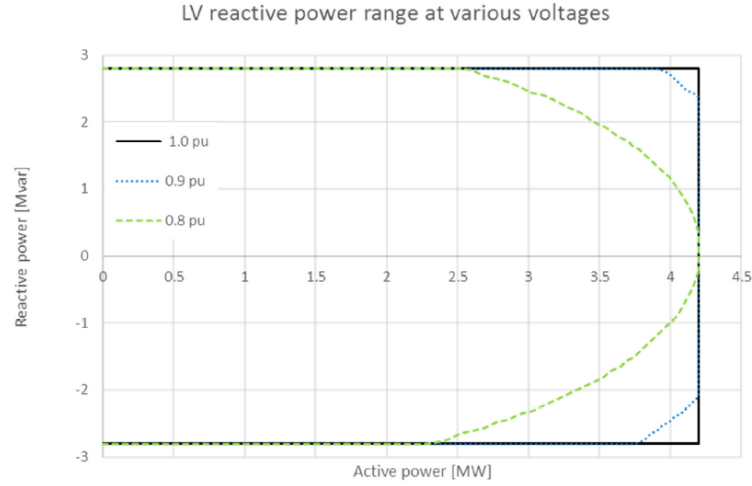LV reactive power range at various voltages

Figure 3.3: Common case for relation between P and Q of WTG
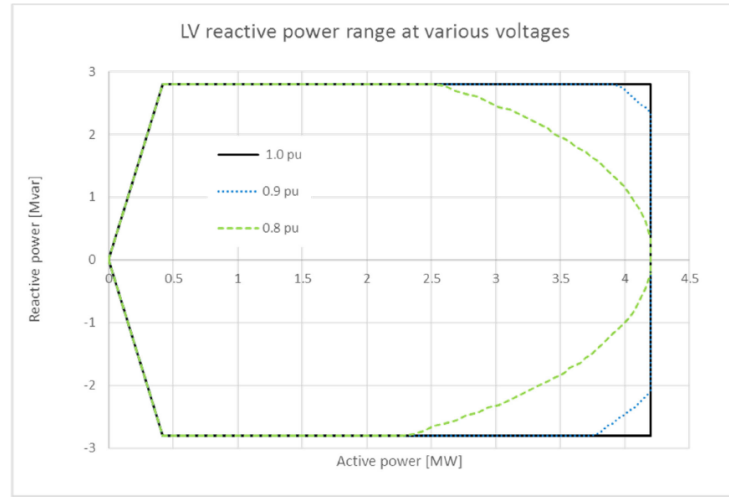

Figure 3.4: Non-ideal case for relation between P and Q of WTG

of the cable. Thus, for each solar farm string an rated power generation of 12 MW is chosen. Therefore, some parts of the day the cable to the PCC will be overloaded with 8 MW. This overloading is needed to give the subgroup, which is responsible for the power flow control, the opportunity to come up with solutions in order to guarantee stability and reliability of active power at the PCC.

Additionally, the type of solar modules has to be chosen. It is decided to implement the Sunpower X-Series solar modules, because these modules have a high efficiency of 22.2% and a sufficient amount of data about the modules is available online [18].

Secondly, in order to supply active power to the case system shown in Fig. A.1, the DC power generated by the solar modules has to be converted into AC power [20]. Thus, in each solar string, DC/AC inverters are implemented in order to apply this conversion. However, during this conversion, reactive power is generated by the inverters [20]. Since no data of the PQ capability curves for these solar modules is available, an approximation for the generated reactive power is made as shown in Eq. 3.4 [6].

$$Q_{gen} = \frac{1}{3} \cdot P_{gen} \tag{3.4}$$

Afterwards, the irradiance in W/m^2 of the location is examined using [4]. When implementing the irradiance profile, a summer model is chosen. This choice is made, since in the summer the irradiance is the most constant and the highest in comparison to the other seasons. This research resulted in a rated irradiance of 800 W/m^2. This value is used in order to calculate the number of modules needed for each solar farm. As

can be seen in [18], the output power of each module at Standard Test Conditions (temperature of 25°C, irradiance of 1000 W/m^2 and an air mass of 1.5 (AM 1.5) is 360W. For the sake of simplicity, the output power is considered to be linearly dependent of the irradiance. Thus, the other two variables, temperature and air mass, are not considered to be of influence in this model. With this assumption, the output power of each module is determined using Eq. 3.6.

$$P_{module_{location}} = \frac{Ir_{location}}{Ir_{STC}} \cdot P_{module_{S}TC} \tag{3.5}$$

In addition, the amount of solar modules needed is calculated

$$N_{modules} = \frac{P_{total}}{P_{module_{location}}} \tag{3.6}$$
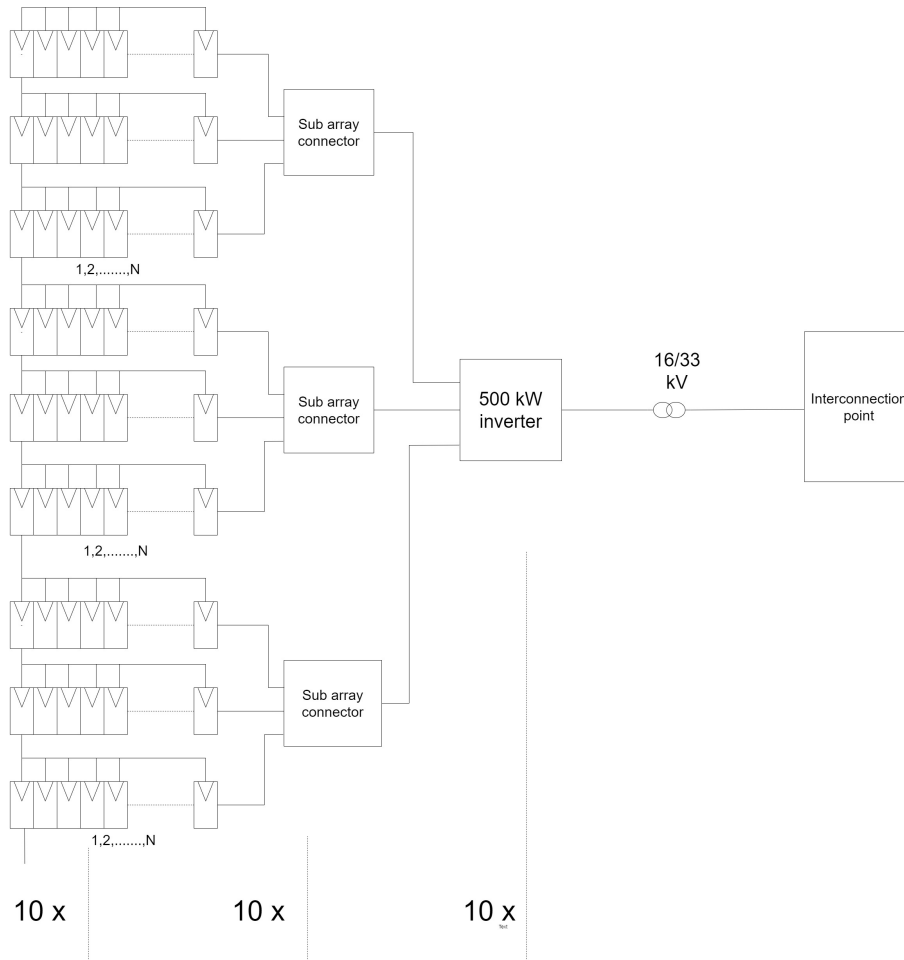
3.3.2. Solar farm overview

Figure 3.5: Overview of solar farm design

3.4. Method to determine model accuracy

MatPower solves the power flows, voltage/current profiles and power losses of nodes in the system, using the Newton Raphson method [19]. To determine if the model was implemented correctly and MatPower is a reliable source tool, the same method was applied with hand calculations. Hereby, the same setpoints for generating strings used for the MatPower code were used to solve the iterative power flow.

Since the system configuration consists of 28 bus bars and 17 generating strings, it could be concluded that performing hand calculations on the entire system would be too intensive for the purpose of this project.
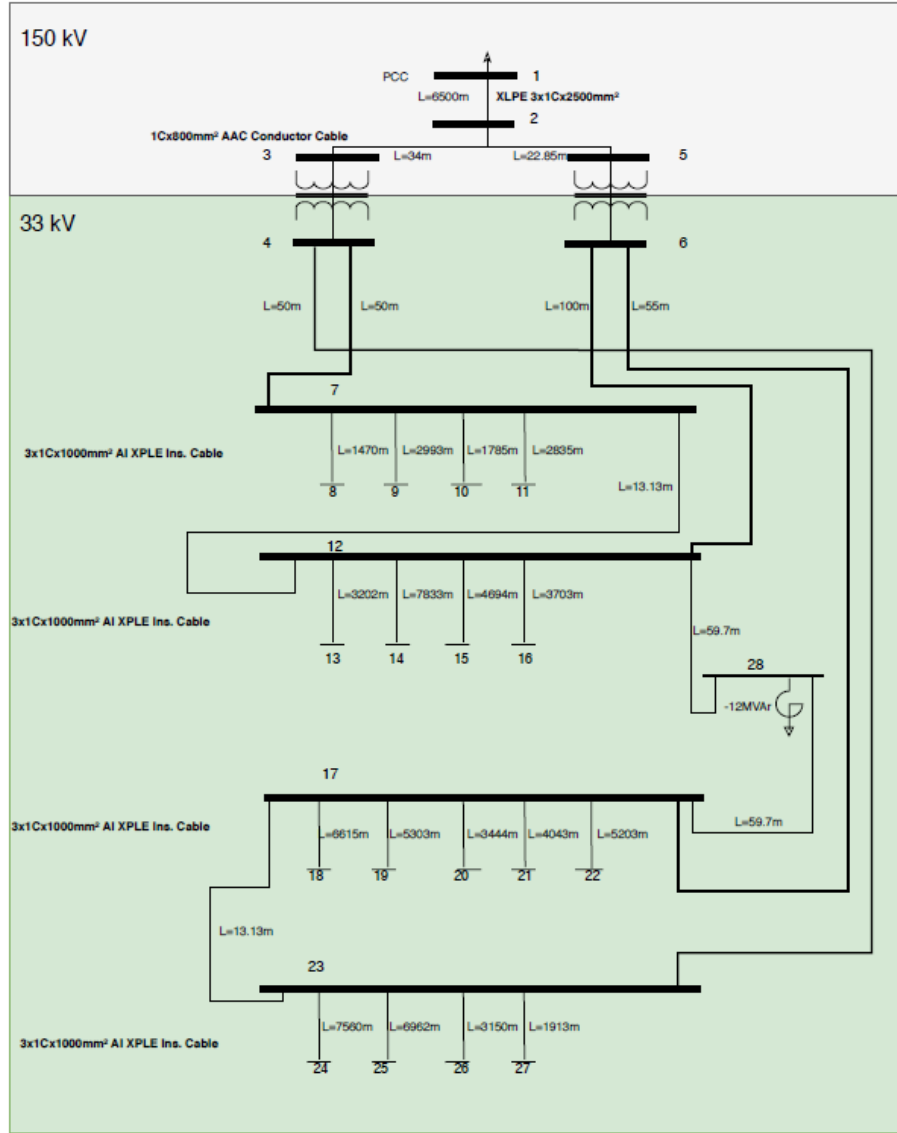
Figure 3.6: Overview of case system used in MatPower

Therefore, it was decided to perform the calculations for one string. This comparison is done for two different reactive power setpoints. The strings chosen were based on the known parameters of the system. When there is a PCC request, reactive power setpoints are sent to the generating strings from the slack node top, to the strings down. Based on this, the voltage profile and current is best known between the WTG and connected bus, e.g. the power flow of branch 7-8 with bus 8 being the WTG, is known after the reactive power demand is known at bus 7. To choose which branch is most relevant to model, the longest branch was chosen since this will cause a higher voltage difference and power loss in the string. With a length of 7561 m, branch 23-24 is tested.
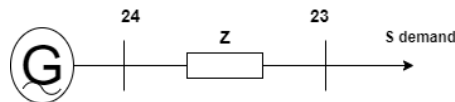

Figure 3.7: Equivalent test model of branch 23-24

Firstly, an equivalent test model is made for the branch, shown in Fig. 3.7. After, an equation is formulated for the active and reactive power through branches Eq. 3.7 and Eq. 3.8. In these equations, i will be the node

for which the power is unknown and n will be the node with known magnitude and angle values. Y_{in} is the admittance value in the admittance matrix for the branch between node i and n. With the Jacobian of Eq. 3.9, Eq. 1.4 is solved. From Eq. 1.4, the power flow is determined. If the mismatch between the calculated power flow and the desired power flow is below a certain threshold, the vector of Eq. 1.4 yields the final solution.

$$P_i = \sum_{n=1}^{N} U_i \cdot U_n \cdot Y_{in} \cdot cos(\delta_i - \delta_n - \theta_{in}) \tag{3.7}$$

$$Q_i = \sum_{n=1}^{N} U_i \cdot U_n \cdot Y_{in} \cdot sin(\delta_i - \delta_n - \theta_{in}) \tag{3.8}$$

$$\begin{vmatrix} \frac{\partial P_i}{\partial \delta_i} & \frac{\partial P_i}{\partial U_i} \\ \frac{\partial Q_i}{\partial \delta_i} & \frac{\partial Q_i}{\partial U_i} \end{vmatrix} \tag{3.9}$$

To solve the equations, all values will be in per unit. To arrive at the known parameter values, the MatPower code ?? is ran with random setpoints centered around 0 and maximum active power generation for each strings. From this test, the values in Tab. ?? are determined. Using Fig. 3.7, in the first test it is assumed that the generation is known, i.e. at bus 24, and the voltage profile at bus 23. In the second test the apparent power demand is known, i.e. at bus 23, and the voltage profile at bus 24. In this manner, the Newton Raphson method is applied for both sides of the model, yielding a more reliable hand calculations result.

Bus number	Voltage magnitude (p.u.)	Voltage angle (degrees)	Y admittance (p.u.)	P (p.u.)	Q (p.u.)	P loss (MW)	Q loss (MVAr)
23	0.9801	18.5814	1.265 - j 7.216158756	0.294	0.000169	0.0607	0.3465
24	0.9776	19.2510	1.265 - j 7.216158756	0.294	0.00023	0.0607	0.3465

For the purpose of this project, a threshold of 0.0001 p.u. for the power flow mismatch is chosen, which is recommended in the lectures of the supervisor for the project. After the final solution is found from Eq. 1.4, the current magnitude and angle is determined. Using Ohm's law, the active and reactive power losses are calculated. Then, the mismatch between the MatPower and hand calculations is analysed to determine if this mismatch can be neglected for the purpose of this project. Based on the total active power, 400 MVA, that theoretically could be provided at the PCC (Bus 1), a maximal mismatch of 1 MW for active power and 1 MVAr for reactive power is chosen. The relative mismatch is 0.25 % which is considered to be a negligible inaccuracy. Furthermore, this mismatch is well within the allowable deviation of the PCC request [15]. The hypotheses is that if the MatPower results are sufficiently close to the hand calculations, MatPower modeling proves to be accurate.

4

Test models for operating conditions

1. Generate loading demands with a normal distribution to test for which PCC requests constraints are violated at each bus and branch of the Single Line Diagram [13]. Unchanged rated power is assumed for each string.

2. Design a daily dispatch for wind profile based on a Weibull PDF.

3. Design a daily dispatch for solar profile based on a Beta PDF. Here, a sunny day with maximal sun hours of the case study area, is assumed.

4. Design a daily dispatch for solar profile based on a Beta PDF, for different spatio-temporal situations. Here, solar profile can be sunny and partly cloudy. More profiles can be added at a later stage.

It should be noted that for each wind/solar dispatch design, it is assumed that the uncorresponding RES system module is inactive. For example, when the PV power generation is modeled with the designed solar irradiance daily dispatch, the WTGs are considered to be inactive. The same counts for the wind daily dispatch design and the inactive PV module. Once each design is tested individually, the dispatches can be combined in a normal random distribution function for wind-and solar PV power active simultaneously.

To test the system behaviour, the model is tested under different operating conditions. A total of 96 dispatches are made; 4 hours divided in 15 minute dispatches. More dispatches will be confusing to analyse and less will be insufficient data. For the correctness of the tests, it is important to disconnect or neglect components that are not part of the components of interest. Therefore, on the voltage profiles, the effects caused by changing the tap position, will be neglected. The tap position is assumed to be fixed and nominal, 1 p.u. This assumption will not be valid anymore for Sec. 4.4.

For each test model the following procedure will be followed:

1. Normal operating conditions:

    (a) Determine maximum active and reactive power for each string.
    (b) Determine most suitable random distribution that can be applied as test model.
    (c) Generate random load demands centered around 0 MVAr. The variation will be 'x' % from the maximum reactive power that each string can generate.
    (d) **Run power flows** for each dispatch. From which:
        i. Determine the voltage profile for each bus.
        ii. Determine the active and reactive power losses for each branch.
        iii. Determine which busses violate physical constraints. Additionally, note which load demands correspond to this behaviour.
        iv. Determine which bus and branches have the highest losses in MVA. Additionally, note which load demands correspond to this behaviour.

v. Determine the power flow through branches 1-2 (to PCC), 4-7(to input of Transformer 1), 4-23(to input of Transformer 2), in Fig. 3.6 and compare it to the branch limit. These branches are the limits for the maximum solar power that can be added to the transmission system.

2. With the load demands close to maximum values known and a better overview of the system behaviour, critical operating condition are determined.

   (a) The distribution will be centered around the average maximum and minimum reactive power of each generating string.

   (b) A small variance is applied to the distribution.

   (c) The test is ran again in a same manner as for normal operating conditions.

   (d) The behaviour for critical operating conditions is determined.

The procedure for the test modeling is depicted in Fig. 4.1 With the output data, plots will be made, depicting the behaviour for each of the possible operating conditions the system can be in.
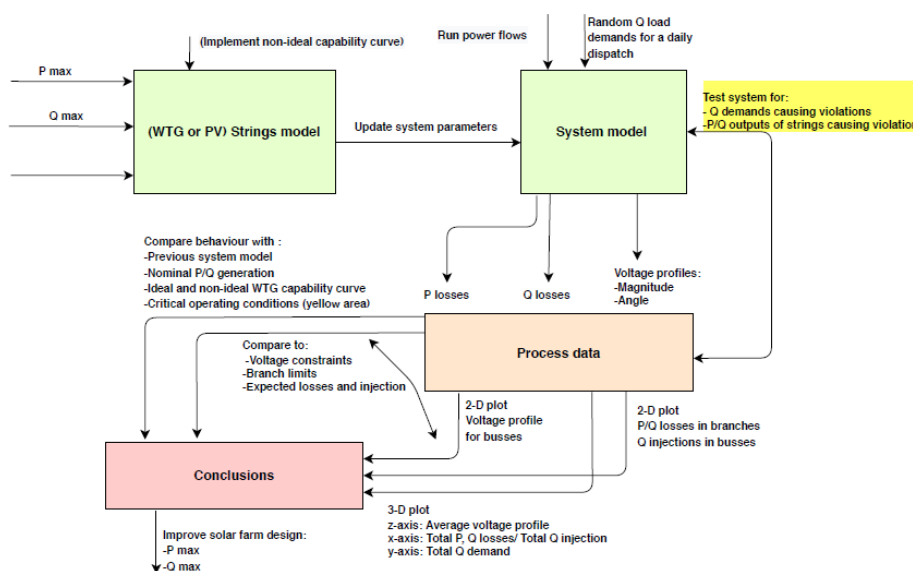

Figure 4.1: Overview of procedure to derive conclusions

The plots make data processing and comparison between current data and data of previous iterations of the system model manageable. Especially, the 3-D plots that for each dispatch, plot the total system losses, average voltage magnitude of all busses and total reactive power demand, depict the total system behaviour for different dispatches. The absolute distance from origin to sample point is determined. The hypotheses is that sample points with highest/lowest voltage magnitudes, have the largest absolute distance to origin. Equivalently, these sample points will have the highest power losses. These sample points form the boundary values for the system. This hypotheses is examined in Chap. 6.

The relation with reactive power demand is still unknown, since the subdivision of demand for the strings is important. If one string is requested with high positive reactive power, and the next string with high negative reactive power, the demand will equal approximately 0 MVAr at the PCC. No conclusion can be derived from this. Therefore, based on the gathered data, power flows are ran again with solely negative or positive demands for each string. Next, to derive reliable conclusion, this is compared to the previously normally distributed load demand, which represent normal operating conditions [8].

4.1. Wind speed profiles and random load demands

4.1.1. Normal wind operating conditions
4.1.2. Extreme wind operating conditions

4.2. Solar irradiance profiles and random load demands

4.2.1. Normal solar operating conditions
4.2.2. Extreme solar operating conditions

4.3. Wind-and solar profiles and random load demands

4.3.1. Normal operating conditions
4.3.2. Extreme operating conditions

4.4. Random tap position and random load demands

4.4.1. Random tap position with fixed wind speed and random load demands
4.4.2. Random tap position with random wind speeds, solar irradiance and random load demands

5

Results

5.1. Determination of model accuracy

5.2. Test Models for operating conditions

5.2.1. Wind farm

5.2.2. Solar farm

5.2.3. Hybrid farm

6
Conclusion

7

Discussion

Bibliography

[1] A.Y. Abdelaziz, Mahmoud M. Othman, M. Ezzat, and A.M. Mahmoud. A novel monte carlo based modeling strategy for wind based renewable energy sources. *Eighteenth International Middle East Power Systems Conference (MEPCON)*, December 2016. DOI: 10.1109/MEPCON.2016.7836897.

[2] European Environment Agency. Making clean renewable energy happen. `https://www.eea.europa.eu/signals/signals-2017/articles/making-clean-renewable-energy-happen`, November 2017. Accessed on 2020-05-10.

[3] S. Conti and S. Raiti. Probabilistic load flow for distribution networks with photovoltaic generators part 1: Theoretical concepts and models. *International Conference on Clean Electrical Power*, May 2007. DOI: 10.1109/ICCEP.2007.384199.

[4] Tu Delft. Dutch pv portal. `https://www.tudelft.nl/en/eemcs/the-faculty/departments/electrical-sustainable-energy/photovoltaic-materials-and-devices/dutch-pv-portal/`, 2020. Accessed on 2020-05-05.

[5] K.C. Divya and P.S. Nagendra Rao. Models for wind turbine generating systems and their application in load flow studies. *Electric Power Systems Research*, 76:844–856, June 2006. DOI: 10.1016/j.epsr.2005.10.012.

[6] ESIG. Reactive power capability and interconnection requirements for pv and wind plants. `https://www.esig.energy/wiki-main-page/reactive-power-capability-and-interconnection-requirements-for-pv-and-wind-plants/`, 2020. Accessed on 2020-05-05.

[7] A. Etxegarai, P. Eguia, E. Torres, G. Buigues, and A. Iturregi. Current procedures and practices on grid code compliance verification ofrenewable power generation. *Renewable and sustainable energy reviews*, February 2015.

[8] A. Etxegarai, P. Eguia, E. Torres, G. Buigues, and A. Iturregi. Incorporation of probabilistic solar irradiance and normally distributed load for the assesment of atc. *8th International Conference on Computing, Communication and Networking Technologies (ICCCNT)*, July 2017.

[9] Andres E. Feijoo and Jose Cidras. Modeling and analysis of wind farms in the load flow analysis. *IEEE Transactions on Power Systems*, 15(1), February 2000. DOI:10.1109/ICCPEIC.2015.7259482.

[10] A.F. Glimm and G.W. Stagg. Automatic calculation of load flows. *AIEEE Transaction on Power Apparatus and Systems*, 76:817–828, October 1957.

[11] K.E. Hagan and O.O. Oyebanjo. A probabilistic forecasting model for accurate estimation of pv solar and wind power generation. *IEEE Power and Energy Conference at Illinois (PECI)*, February 2016.

[12] I.Munteanu. *Optimal control of wind energy systems: towards a global approach.*

[13] K.N. VWHV-UO-3.2.OS-OWN-E0014032-E01-FA0-000001-E-overall Single Line. ABB Power Grids The Netherlands B.V., 2020. Approved by Gregory Kinburn ABB PGGI Rotterdam.

[14] F.H. Mahmood, A.K. Resen, and A.B. Khamees. Wind characteristic analysis based on weibull distribution of al-salman site, iraq. *Energy reports*, February 2020.

[15] P. Mayer. Steady-state grid compliance report. July 2019.

[16] P. Priyadharshini and M. Mohamed Thameem Ansari. Modeling and analysis of wind farms in load flow studies. *International Conference on Computation of Power, Energy, Information and Communication (ICCPEIC)*, April 2015. DOI: 10.1109/ICCPEIC.2015.7259482.

[17] R. Ramakrishna, A. Scaglione, V. Vittal, E. Dall'Anese, and A. Bernstein. A model for joint probabilistic forecast of solar photovoltaic power and outdoor temperature. *IEEE Transactions on Signal Processing*, 67(24), November 2019.

[18] Sunpower. Sunpower x-series. `https://us.sunpower.com/sites/default/files/media-library/data-sheets/sunpower-x-series-residential-solar-panels-x22-360-datasheet-514618-revc.pdf`, September 2017. Accessed on 2020-05-05.

[19] W.F. Tinney and C.E. Hart. Power flow solution by newton's method. *IEEE Transaction on Power Apparatus and Systems*, PAS-86(11):1449–1460, November 1967.

[20] A. Cabrera Tobar, E. Bullich-Massague, M. Arruages-Penalba, and O. Gomis-Bellmunt. Reactive power capability analysis of a photovoltaic generator for large scale power plants. *5th IET International Conference on Renewable Power Generation (RPG)*, 2016. DOI: 10.1049/cp.2016.0574.

[21] S.L. Walker. Building mounted wind turbines and their suitability for the urban scale—a review of methods of estimating urban wind resource. *Energy and buildings*, August 2011.

[22] L. Webb. How has the renewable energy market changed in the last decade? `https://www.nesgt.com/blog/2020/01/how-has-the-renewable-energy-market-changed-in-the-last-decade`, January 2020. Accessed on 2020-05-01.

[23] Z-S. Zhang, Y-Z. Sun, J. Lin, L. Cheng, and G-J. Li. Versatile distribution of wind power output for a given forecast value. *IEEE Power and Energy Society General Meeting*, July 2012.

[24] R. D. Zimmerman and C.E. Murillo-Sánchez. Matpower user's manual. 2019.

[25] N.A. Zulkilfi, N.M.M. Razali, M. Marsadek, and A.K. Ramasamy. Probabilistic analysis of solar photovoltaic output based on historical data. *IEEE 8th International Power Engineering and Optimization Conference (PEOCO2014)*, March 2014.

A

Appendix

A.1. Additional overviews

A.2. Cable modeling

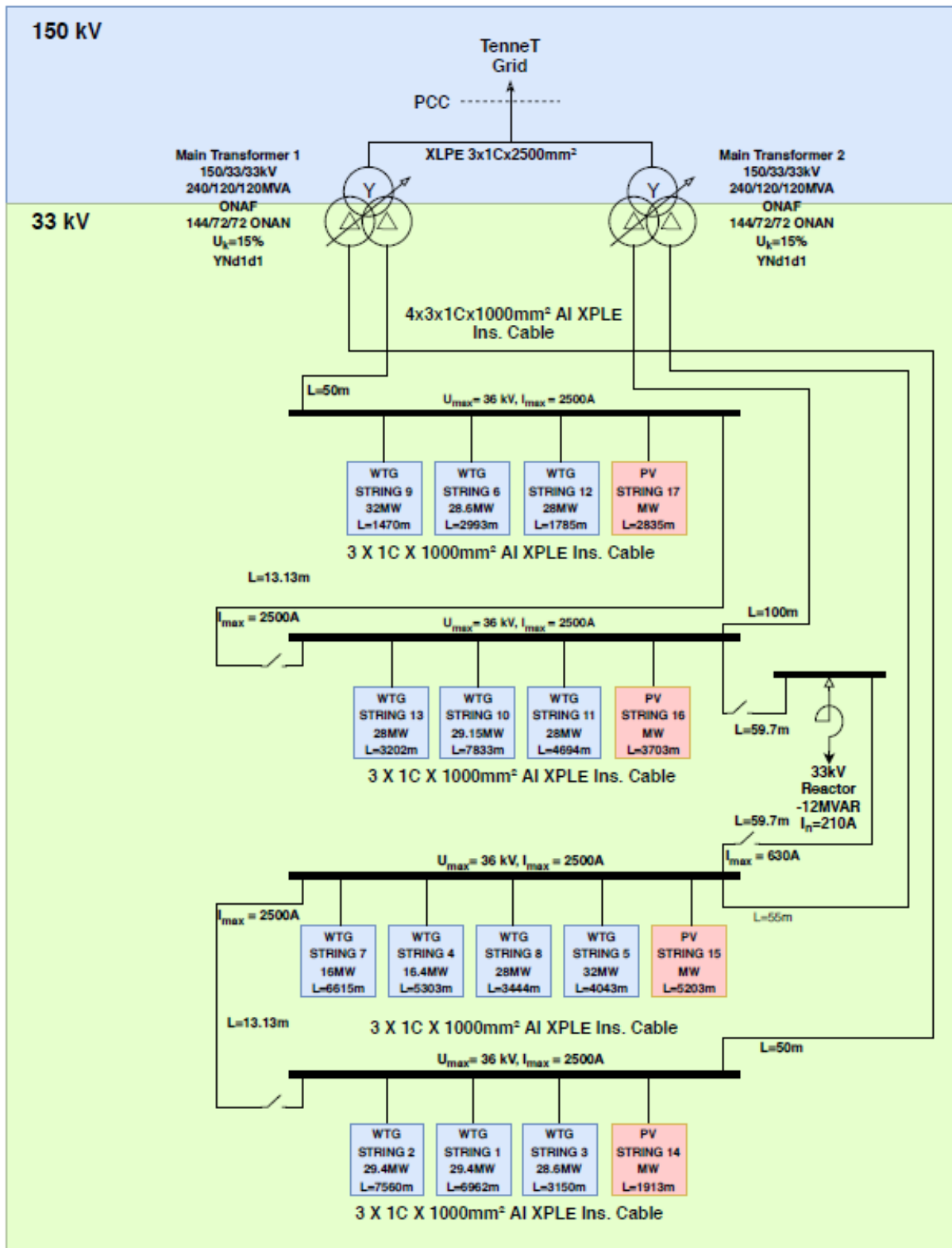**A.2.1. Cable configurations**

A.2.2. Branch calculations

A.3. MatLab codes

Figure A.1: Schematic of case system

String	Index	Address	Enercon Type	P_nom [kW]	P_string [MW]
String 1	1	A27-01	E-138	4200	29,4
	2	A27-02	E-138	4200	
	3	A27-03	E-138	4200	
	4	A27-04	E-138	4200	
	5	A27-05	E-138	4200	
	6	A27-06	E-138	4200	
	7	A27-07	E-138	4200	
String 2	8	A27-11	E-138	4200	29,4
	9	A27-12	E-138	4200	
	10	A27-13	E-138	4200	
	11	A27-14	E-138	4200	
	12	A27-15	E-138	4200	
	13	A27-16	E-138	4200	
	14	A27-17	E-138	4200	
String 3	15	A27-08	E-138	4200	28,6
	16	A27-09	E-138	4200	
	17	A27-10	E-138	4200	
	18	ADW-05	E-115	4000	
	19	ADW-06	E-115	4000	
	20	ADW-07	E-115	4000	
	21	ADW-08	E-115	4000	
String 4	22	ADW-01	E-138	4200	16,4
	23	ADW-02	E-138	4200	
	24	ADW-03	E-115	4000	
	25	ADW-04	E-115	4000	
String 5	26	ADW-11	E-126	4000	32
	27	ADW-12	E-126	4000	
	28	ADW-13	E-126	4000	
	29	ADW-14	E-126	4000	
	30	ADW-15	E-126	4000	
	31	ADW-16	E-126	4000	
	32	ADW-17	E-126	4000	
	33	ADW-18	E-126	4000	
String 6	34	ADO-01	E-138	4200	28,6
	35	ADO-02	E-138	4200	
	36	ADO-03	E-138	4200	
	37	ADO-04	E-115	4000	
	38	ADO-05	E-115	4000	
	39	ADO-06	E-115	4000	
	40	ADO-07	E-115	4000	
String 7	41	ADW-19	E-126	4000	16
	42	ADW-20	E-126	4000	
	43	ADO-20	E-126	4000	
	44	ADO-22	E-126	4000	
String 8	45	ADO-14	E-126	4000	28
	46	ADO-15	E-126	4000	
	47	ADO-16	E-126	4000	
	48	ADO-17	E-126	4000	
	49	ADO-18	E-126	4000	

Figure A.2: Overview of different Enecon WTG types connected to each string of the transmission system [15] [13].
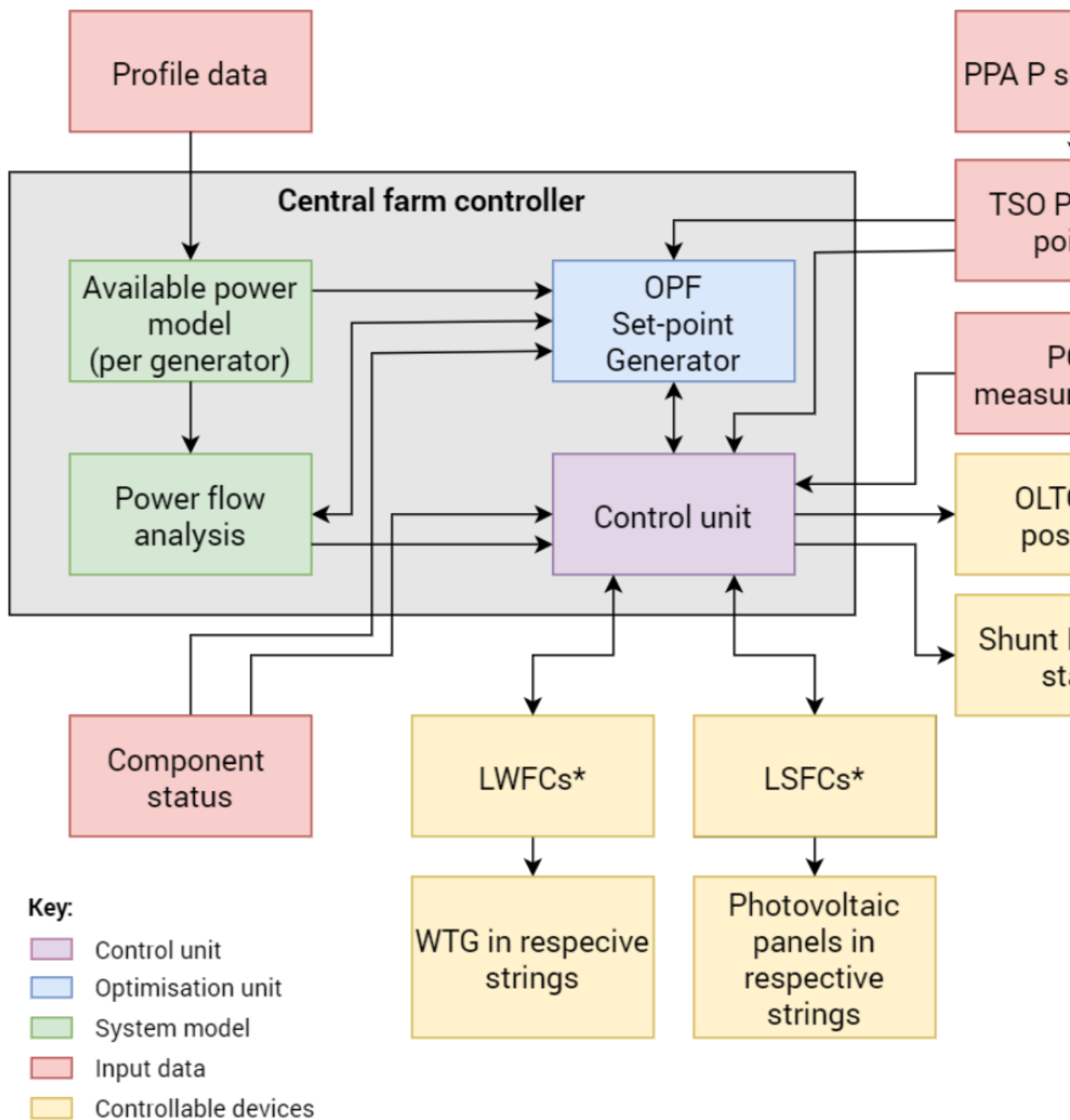
Figure A.3: Overview of interaction between the three components that together form the optimisation unit.
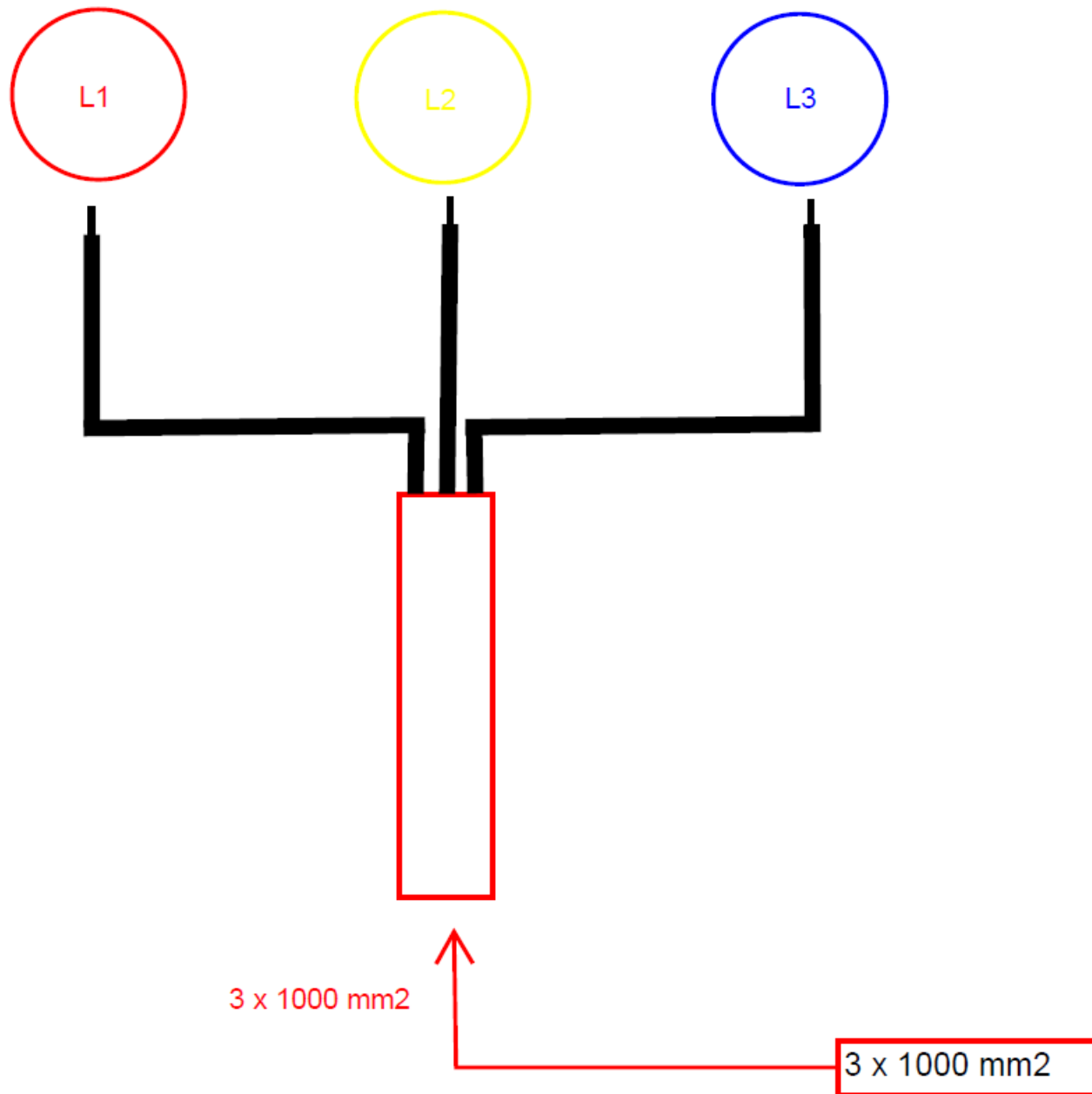
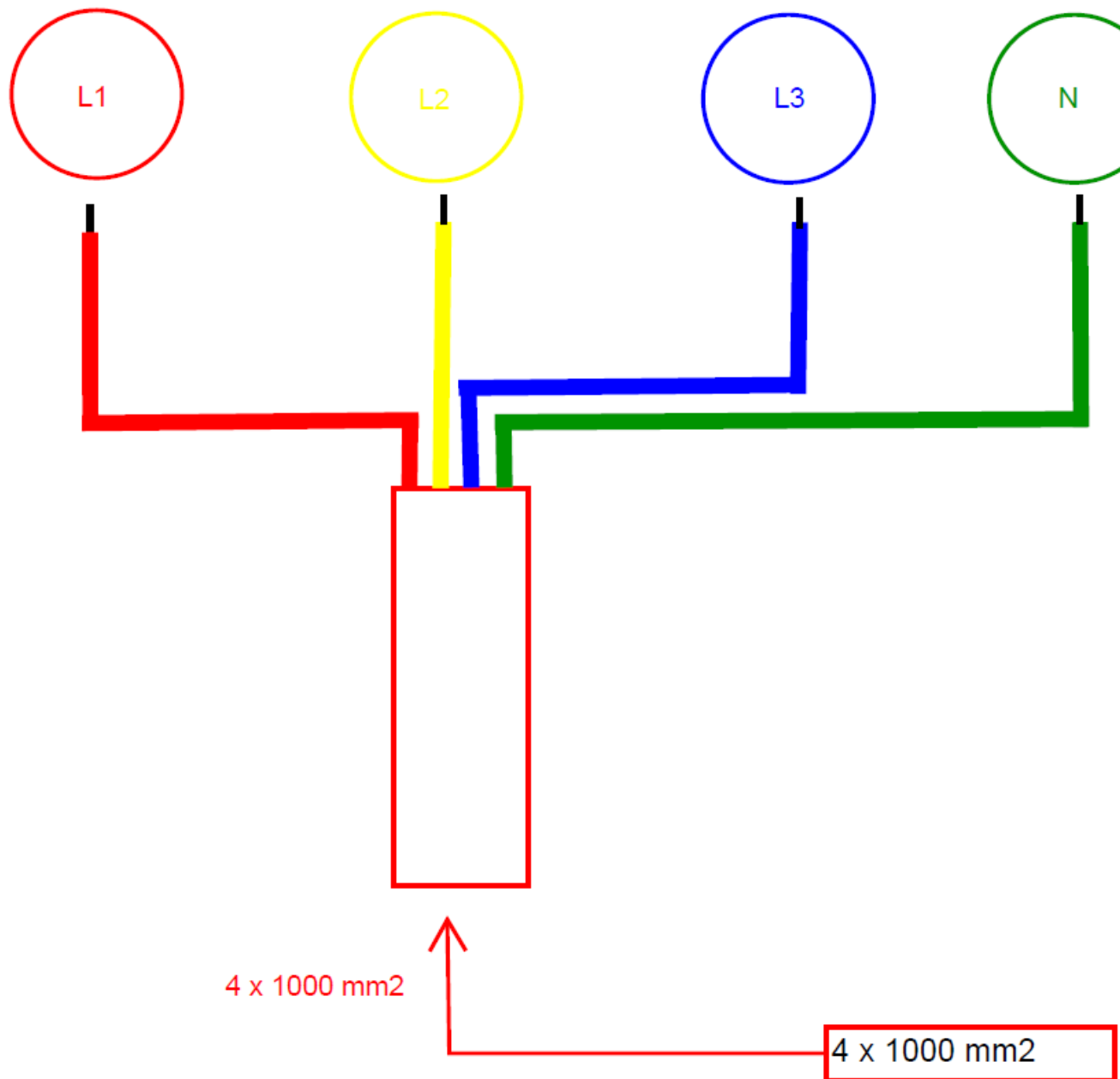Figure A.4: Cable configuration for a 3x1000mm2 XLPE Al cable. Data from [15].

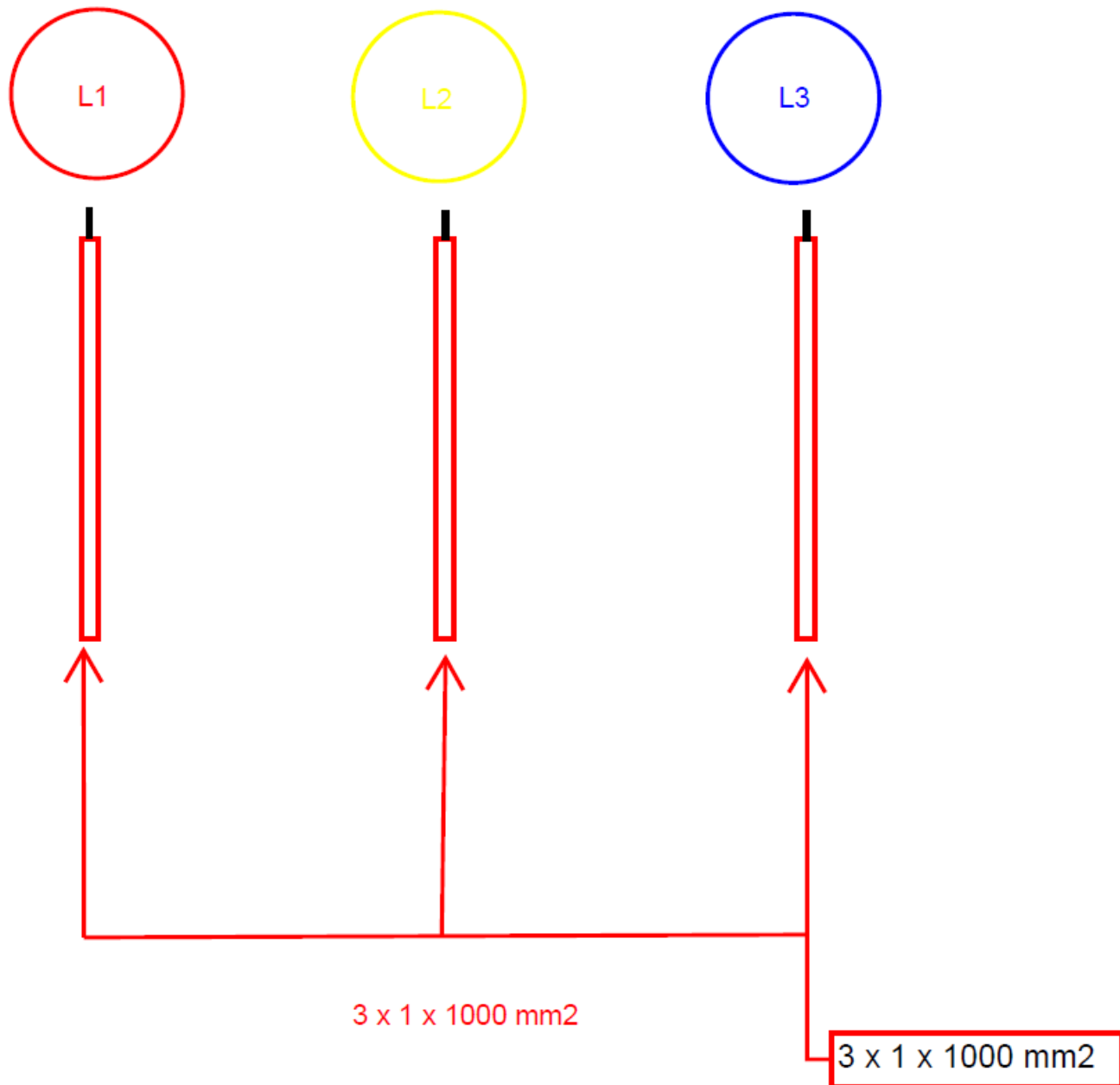Figure A.5: Cable configuration for a 4x1000mm2 XLPE Al cable. Data from [15].

Figure A.6: Cable configuration for a 3x1x1000mm2 XLPE Al cable. Data from [15].